https://doi.org/10.15407/ujpe71.8.652

O.M. MALININ, A.O. MALININA, O.K. SHUAIBOV,
K.B. MOLNAR, O.Y. MYNIA, R.V. HRYTSAK, M.O. MARGITYCH
Uzhgorod National University
(54, Voloshyna Str., Uzhgorod 88000, Ukraine; e-mail: alex.malinin@uzhnu.edu.ua)

PARAMETERS AND RADIATION PROPERTIES OF PLASMA OF BARRIER DISCHARGE BASED ON A MIXTURE OF MERCURY DIIODIDE, DIBROMIDE, AND DICHLORIDE VAPORS WITH HELIUM

The parameters of the plasma of the pulse-periodic nanosecond barrier discharge based on a vapor mixture of three mercury dihalides (HgI_2, $HgBr_2$, and $HgCl_2$) and helium at atmospheric pressure, as well as the spectral and energy properties of its radiation, have been studied. Simultaneous radiation emission of spectral bands was detected in the violet-blue (λ_{max} = 444 nm), blue-green (λ_{max} = 502 nm), and green (λ_{max} = 557 nm) spectral intervals. The mechanism of formation of exciplex molecules of mercury monohalides (HgI^*, $HgBr^*$, and $HgCl^*$) was discussed. The rate constants for the excitation of exciplex molecules of mercury monohalides were determined. The optimal values of the reduced electric field strength at which the radiation power in the violet-blue, blue-green, and green spectral ranges is maximum, with the emission maxima at wavelengths of 444, 502, and 557 nm, were found. On the basis of performed research, a new excilamp can be created that simultaneously emits three spectral bands in the visible spectral intervals and can be used in scientific research and medicine, for technological renewal and development of greenhouse farming, in biotechnology, for more effective management of photosynthesis, growth, and development of plants and algae, as well as in seawater desalination technology and for more energy-efficient drying methods in industry.

Keywords: nanosecond barrier discharge, radiation of exciplex molecules, plasma parameters, mercury monohalides, helium.

1. Introduction

The study of the parameters of barrier discharge plasma and the optical properties of its radiation is important for both improving the existing and creating new radiation sources [1]. Plasma based on mixtures of vapors of three mercury dihalides (mercury dibromide $HgBr_2$, diiodide HgI_2, and dichloride $HgCl_2$) with atomic and molecular gases can be an effective exciplex source of three-band coherent and spontaneous emission in the violet-blue, blue-green, and green spectral intervals, with the maxima at wavelengths of 444, 502, and 557 nm, respectively [2, 3]. The optical characteristics of radiation emitted by mixtures of vapors of separate dihalides of metals from the second group of the periodic table

Citation: Malinin O.M., Malinina A.O., Shuaibov O.K., Molnar K.B., Mynia O.Y., Hrytsak R.V., Margitych M.O. Parameters and radiation properties of plasma of barrier discharge based on a mixture of mercury diiodide, dibromide, and dichloride vapors with helium. *Ukr. J. Phys.* **71**, No. 8, 652 (2026). https://doi.org/10.15407/ujpe71.8.652.

of chemical elements with gases were determined in our studies [4–13], where the possibility of creating gas-discharge excilamps emitting separate bands in the visible spectral range and their possible application in scientific research, medicine, for technological renewal and development of greenhouse farming, in biotechnology, for more effective management of photosynthesis, growth, and development of plants and algae was determined.

In recent years, studies reported in Ref. [14, 15] revealed new possibilities for the application of radiation of separate spectral bands in the visible interval. In Ref. [14], the possibility of using light of certain wavelengths for the manufacture of functional molecules in the living environment was revealed, which opens a new technology for precise manipulation with human cells for point therapy. In the studies of scientists from the Massachusetts Institute of Technology [15], it was found that light can evaporate water without using heat. Their study showed that when exposed to light of certain wavelengths, water can evaporate, avoiding heating. In experiments carried out by the cited researchers, it was found that light, when incident on the surface of water, can directly stimulate the release of water molecules, thus causing them to evaporate regardless of the temperature. This discovery has significant implications. It could help resolve existing discrepancies in the data on moisture absorption by clouds, which is important for more accurate predictions of climate change. It also opens up new opportunities for the development of technologies, such as seawater desalination or more energy-efficient drying methods in industry.

In Ref. [16], it was shown that the key current problem with exciplex emitters is improving the utilization of their components. The cited authors proposed a strategy for constructing exciplex emitters with three active components. It is believed that the introduction of multiple excitation channels can effectively improve the utilization of various molecules in exciplex emitters; it also proves the advantage of the three-component exciplex strategy for the further development of the gas-discharge exciplex emitters.

This work is devoted to the study of the optical (spectral and energy) characteristics of radiation in the wavelength range of 350–700 nm emitted by the gas-discharge plasma of a single-barrier discharge initiated by a pulse-periodic voltage of nanosecond duration in a mixture of vapors of three mercury dihalides

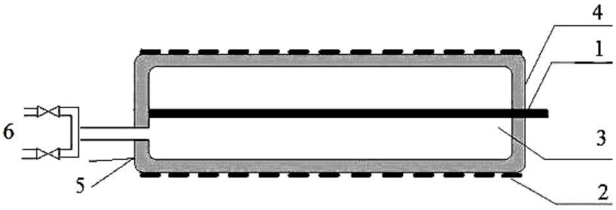

Fig. 1. Schematic diagram of emitter: internal electrode (*1*), external (mesh) electrode (*2*), discharge gap (*3*), quartz glass (*4*), thermocouple (*5*), valves of the pumping and gas supply system (*6*)

($HgI_2 : HgBr_2 : HgCl_2$) with helium, as well as to the determination of plasma parameters, the analysis of the mechanism of formation of exciplex molecules of mercury monohalides (HgI^*, $HgBr^*$, $HgCl^*$), and the determination of the reduced electric field strength at which the radiation power is maximum in the violet-blue, blue-green, and green spectral intervals, with emission maxima at wavelengths of 444, 502, and 557 nm.

2. Equipment and Research Method

The optical properties of radiation emitted by barrier discharge plasma in a mixture of mercury diiodide, dibromide, and dichloride vapors with helium were studied in a device (emitter), the schematic diagram of which is presented in Fig. 1. Quartz glass served as a barrier. The barrier discharge plasma of the examined mixture was created in the interelectrode gap (*3*) in a cylindrical device made of a quartz glass tube (KU-2 quartz glass) (*4*) with an outer diameter of 8 mm and a length of 8 cm. A molybdenum electrode (*1*) with a diameter of 0.5 mm was located inside the tube along its axis. The discharge gap (*3*) was 3.25 mm. The outer electrode (7 cm long) (*2*) was made of a metal mesh (stainless steel); the radiation transmission coefficient of the mesh was 70%.

The discharge was powered by a generator of pulse-periodic nanosecond pulses (Fig. 2). During the experiments, the amplitudes of the voltage and current pulses varied within the ranges of 1.5–4.2 kV and 0.03–0.1 A, respectively, the pulse repetition frequency was 6 kHz, the duration of the voltage pulses at half-maximum was 180 ns, and the durations of current pulses were 25 and 75 ns (the current pulses were double with different polarity; their complicated shape was caused by the recharging of the

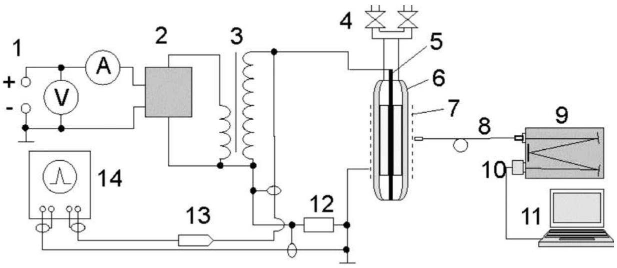

Fig. 2. Schematic diagram of the system for registrating optical and electrical characteristics in the pulse-periodic voltage mode: DC source (*1*), generator (*2*), high-voltage transformer (*3*), pumping and gas supply system (*4*), electrode (*5*), quartz tube (*6*), external (mesh) electrode (*7*), optical fiber (*8*), monochromator (*9*), CCD detector (*10*), personal computer (*11*), shunt (*12*), voltage divider (*13*), oscilloscope (*14*)

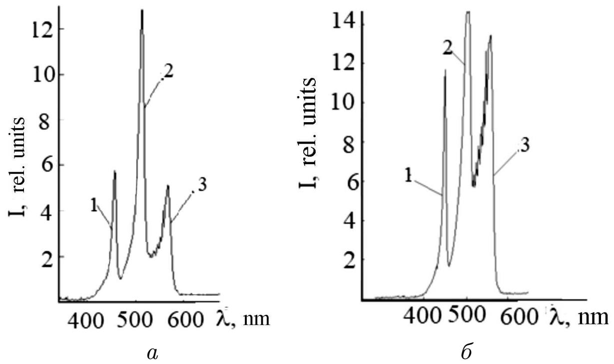

Fig. 3. Emission spectra of the $HgI_2:HgBr_2:HgCl_2:He$ vapor mixture at total pressures of 104 (*a*) and 129 kPa (*b*). Systems of spectral bands of the $B^2\Sigma^+_{1/2} \rightarrow X^2\Sigma^+_{1/2}$ electronic-vibrational transition of exciplex molecules HgI* (λ_{max} = 444 nm) (*1*), HgBr* (λ_{max} = 502 nm) (*2*), and HgCl* (λ_{max} = 557 nm) (*3*). The voltage amplitude is 3.5 kV, and the pulse repetition frequency is 6 kHz

"insulator–plasma" circuit [7]). Radiation was emitted from the central region of the interelectrode gap and analyzed in the visible and near-UV spectral regions using the optical system of the experimental setup, namely, a spectrometer of the SL40-2-1024USB series of a compact two-channel spectrum analyzer (Fig. 2). The spectral resolution of the SL40-2 spectrometer was <1.5 nm at the wavelength $\lambda = 450$ nm (a diffraction grating 600 lines/mm) and <0.8 nm at the wavelength $\lambda = 280$ nm (a diffraction grating 1200 lines/mm).

The voltage and discharge current pulses of the radiation source were registered using a C1-72 oscilloscope. A signal was supplied from a voltage divider and an integrating circuit of a calibrated Rogowski belt. The average radiation power was measured using a Quartz-01 device.

The examined mixture was prepared directly in the interelectrode gap. Mercury dihalides (mercury diiodide, mercury dibromide, and mercury dichloride), 80 mg each, were preliminarily loaded into the interelectrode gap. The surfaces of the elements in the internal tube volume were degassed by heating the volume at a temperature of 50 °C and pumping it to a residual gas pressure of 1.3×10^{-1} Pa for 2 h. The partial pressure of HgI_2, $HgBr_2$, and $HgCl_2$ vapors in the mixture was created by heating the mixture owing to the dissipation of the pulse-periodic discharge energy. Its measurement was carried out according to the temperature of the coldest part of the tube and by linear interpolation of the reference data [17]. The partial pressure of helium was measured by means of a calibrated membrane manometer.

3. Research Results and Their Discussion

In Figs. 3, *a* and 3, *b*, the emission spectra of the barrier discharge plasma based on a mixture of the mercury diiodide, dibromide, and dichloride vapors with helium are presented. The total pressure of the mixtures was 104 and 129 kPa, respectively. The repetition rate of pump pulses was 6 kHz, and the voltage amplitude across the electrodes was 3.5 kV.

The emission spectrum is characterized by the presence of the spectral band systems of the electronic-vibrational transition $B^2\Sigma^+_{1/2} \rightarrow X^2\Sigma^+_{1/2}$ of exciplex molecules HgI*, HgBr*, and HgCl* with emission maxima at the wavelengths λ = 444 (*1*), 502 (*2*), and 557 nm (*3*), respectively, with a steep intensity increase of these spectral bands on the long-wavelength side and a slow decline on the short-wavelength side [18]. The spectral bands overlap in the wavelength interval of 380–580 nm. With an increase in the partial pressure of helium from 104 (Fig. 3, *a*) to 129 kPa (Fig. 3, *b*), a growth of radiation intensity in the spectral bands was observed (the maximum increase took place for the spectral band with the maximum at $\lambda = 502$ nm). As the partial pressure of helium grew further, the intensity of spectral bands decreased.

With the change in the repetition rate of pump pulses from 6 to 8 kHz, the shapes, widths, and positions of emission maxima in the spectral bands did not change; only their intensities and the intensity ratios within the spectral bands.

To determine the conditions under which the highest specific power in the spectral bands of radiation, with radiation maxima at the wavelengths $\lambda = 444$, 502, and 557 nm, is observed, we studied the integral radiation properties. The dependences of the average radiation power on the partial pressure of the helium buffer gas, the mixture temperature, and the voltage amplitude of the external pump source are presented in Figs 4, 5, and 6, respectively. As the helium pressure p grows, the average radiation powers in the spectral bands of the exciplex molecules $HgBr^*$, $HgCl^*$, and HgI^* increase and reach maximum values of 7.3, 7.2, and 6 mW, respectively, at $p = 128$ kPa; then, these quantities decrease (Fig. 4). If the mixture temperature increases from 100 °C, the average radiation powers in the three indicated spectral bands of exciplex molecules also increase and reach maximum values at a temperature of 150 °C; then, they also decrease (Fig. 5). Similar dependences are observed for the voltage pulse amplitude U (Fig. 6): the average radiation powers reach maximum values of 7.3, 7.2, and 6 mW, respectively, at $U = 3.5$ kV.

The following regularity is observed: the values of the radiation power in the spectral bands of molecules do not coincide at the maxima of the corresponding dependences (Figs 4–6). This circumstance may be associated with the influence of the relaxation kinetics of vibrational states in the B and X states of the $HgBr^*$, $HgCl^*$, and HgI^* molecules on the width of their spectral emission bands, thus affecting the emitted power.

3.1. Plasma parameters

The study of plasma parameters in the case of the mixture under atmospheric pressure is a difficult task in both methodological and technical aspects [19]. In this regard, we used a theoretical method that has been successfully tested for discharges based on other mixtures of dihalide vapors with gases [5–8, 10]. According to this method, the parameters of gas-discharge plasma were determined on the basis of the known electron energy distribution function (EEDF). To determine the EEDF, the kinetic Boltzmann equation for quasi-stationary electron energy distribution functions is used [20].

In the integral of electron collisions with mercury dibromide, diiodide, and dichloride molecules, the following processes were taken into account: vibra-

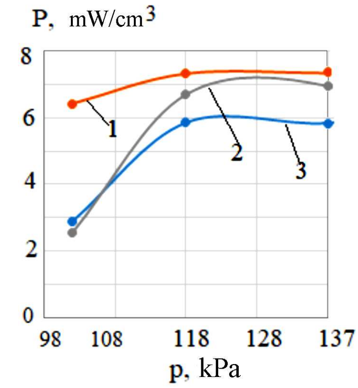

Fig. 4. Dependences of the average radiation power P on the partial helium pressure p: $HgBr^*$ (*1*), $HgCl^*$ (*2*), HgI^* (*3*). The voltage amplitude is 3.5 kV, and the pulse repetition frequency is 6 kHz

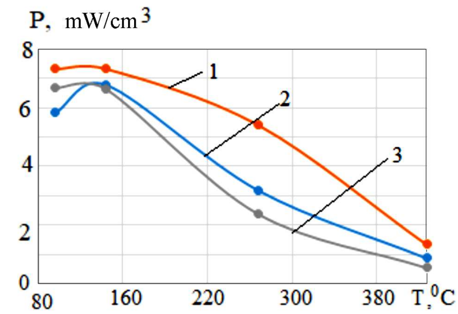

Fig. 5. Dependences of the average radiation power P on the mixture temperature T: $HgBr^*$ (*1*), HgI^* (*2*), $HgCl^*$ (*3*). The voltage amplitude is 3.5 kV, the pulse repetition frequency is 6 kHz, and the partial helium pressure is 128 kPa

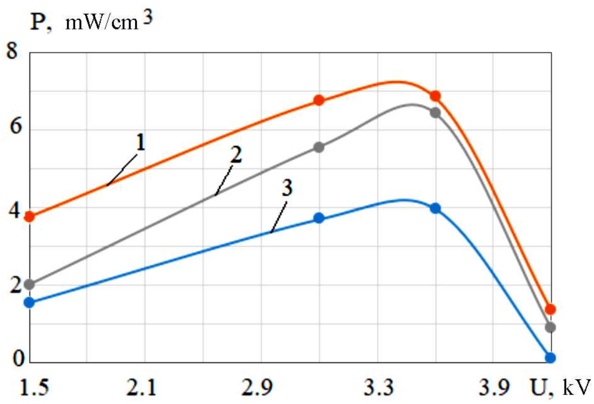

Fig. 6. Dependences of the average radiation power P on the pulse-voltage amplitude U: $HgBr^*$ (*1*), $HgCl^*$ (*2*), HgI^* (*3*). The pulse repetition frequency is 6 kHz, the mixture temperature is 150 °C, and the partial helium pressure is 128 kPa

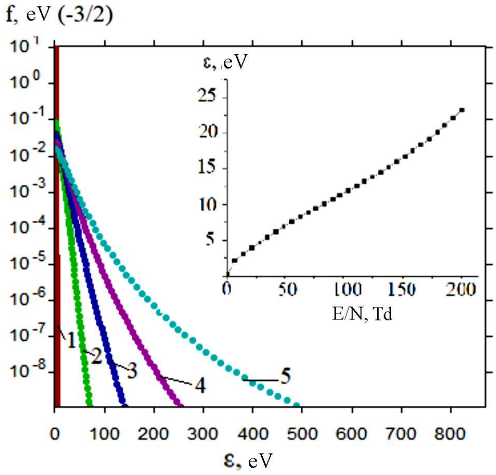

Fig. 7. Electron energy distribution functions (EEDFs) f for the vapour mixture $HgI_2 : HgBr_2 : HgCl_2 : He$ = 126.2 Pa : : 449.4 Pa : 505.6 Pa : 128000 Pa at the total mixture pressure P = 129131.2 Pa for E/N = 1 (*1*), 50.8 (*2*), 100 (*3*), 150 (*4*), and 200 Td (*5*). Inset: the dependence of the average electron energy on the parameter E/N

Table 1. **Electron transport characteristics: average energy ε, temperature T, drift velocity v_{dr}, and concentration N_e in the discharge in the vapor mixture $HgI_2 : HgBr_2 : HgCl_2 : He$ = 126.2 Pa : : 449.4 Pa : 505.6 Pa : 128000 Pa with the total mixture pressure P = 129131.2 Pa**

E/N, Td	ε, eV	T, K	$v_{dr.}$, m/s	N_e, m^{-3}
49	6.88	79808	1.1×10^5	4.52×10^{16}

tional excitation of $HgBr_2$ molecules, excitation of the $HgBr_2(D)$ state, dissociative excitation of mercury monobromide molecules (the $X^2\Sigma^+_{1/2}$ and $B^2\Sigma^+_{1/2}$ states), electron attachment and ionization, dissociative excitation of the $B^2\Sigma^+_{1/2}$ state of mercury monoiodide molecules, ionization of mercury diiodide molecules, dissociative excitation of the $B^2\Sigma^+_{1/2}$ state of mercury monochloride molecules, ionization of mercury dichloride molecules, elastic scattering, excitation of the electronic levels of helium atoms (2^3S), and ionization of helium atoms. Data on the absolute values of the effective cross-sections for those processes, as well as their dependences on electron energies, were taken from references [21–24].

The electric field strength E in the plasma was calculated using the formula

$$E = U_{pl.}/d,$$

where $U_{pl.}$ is the voltage across the plasma, and d is the discharge gap width. The voltage $U_{pl.}$ across the plasma was determined from Kirchhoff's second law using experimentally measured values of the voltage U applied to the electrodes of the gas-discharge cell as a function of time, as well as the voltage drop

$$U_{pl.} = U - U_{dl.}$$

across the insulator capacitance. The voltage $U_{dl.}$ was calculated using the transferred charge Q and the dielectric barrier capacitance C_d,

$$U_{dl.} = Q/C_d.$$

The charge transferred in the circuit was determined by integrating the current $I(t)$ and taking into account the initial conditions:

$$Q(t) = \int_0^t I(t)dt + Q_0,$$

where $Q_0 = Q(t = 0)$.

As a result, the electric field strength E and the reduced electric field in the plasma, E/N, at which the maximum radiation powers in the spectral bands of mercury monoiodide, monobromide, and monochloride exciplex molecules were observed in the experiment (at λ_{max} = 444, 502, and 557 nm, respectively), had the values E = 1076923 V/m and E/N = 49 Td at the total concentration of mixture components $N = 2.2 \times 10^{25}$ m^{-3}. They were determined using the method described in Ref. [25].

In Fig. 7, characteristic profiles of the EEDF for the $HgBr_2$–HgI_2–$HgCl_2$–He mixture are shown for the different values of the parameter E/N within the range of 1–200 Td. An increase in the E/N-value leads to an increase in the number of "fast" electrons in the discharge. The average electron energy increases almost linearly from 0.23 to 23.2 eV when the reduced electric field strength increases from 1 to 200 Td (Fig. 7, inset). For the reduced electric field strength E/N = 49 Td at which the highest power was achieved in the experiment, the maximum electron energy was 84.32 eV.

Under the experimental conditions, for the reduced electric field strength E/N = 49 Td, the average electron energy was 6.88 eV, the temperature was 79808 K, and the electron drift velocity was 1.1×10^5 m/s (Table 1). The electron concentration at the surface of the inner electrode was 4.52×10^{16} m^{-3} at a current density of 796.18 A/m^2.

In Fig. 8, the dependences of the specific power of discharge losses due to elastic and inelastic collision processes of electrons with mercury dibromide, mercury diiodide, and mercury dichloride molecules and helium atoms on the reduced electric field strength in the plasma are shown for the mixture $HgI_2 : HgBr_2 : HgCl_2 : He = 126.2$ Pa : 499.4 Pa : 505.6 Pa : 128000 Pa at a total pressure of 129131.2 Pa. It is observed that the specific power increases as the reduced electric field strength grows. For inelastic electron collisions with plasma components, the specific power of discharge losses is larger than that in elastic processes. It reaches a value of 0.1133×10^{-12} eV m^3/s at $E/N = 200$ Td (Fig. 8).

In Table 2, the values of the specific power of discharge losses in elastic and inelastic processes of electron collisions with mercury dibromide, mercury diiodide, and mercury dichloride molecules and helium atoms are presented. For inelastic electron collisions with plasma components, the corresponding values are approximately 34 times larger than those for elastic ones.

The distribution of specific discharge power losses among the processes of electron collisions with mercury dihalide molecules and helium atoms is presented in Fig. 9. The values of specific discharge power losses during dissociative excitation of mercury monoiodide, monobromide, and monochloride exciplex molecules by electrons increase with the increasing reduced electric field strength. They reach maximum values of 30.2%, 12.6%, 46.2%, 2.8% and 1.1% at $E/N = 7.9$, 21.6, 28.4, 14.7, and 21.6 Td for the $X^2\Sigma^+_{1/2}$ and $B^2\Sigma^+_{1/2}$ electronic states of mercury monobromide molecules, the $HgBr_2\,(D)$ state of mercury dibromide molecules, and the $B^2\Sigma^+_{1/2}$ states

Table 2. **Specific powers of discharge losses in elastic and inelastic electron collisions with dihalide molecules and helium atoms in the vapor mixture $HgI_2 : HgBr_2 : HgCl_2 : He = 126.2$ Pa : 449.4 Pa : 505.6 Pa : 128000 Pa with the total mixture pressure $P = 129131.2$ Pa at the reduced electric field strength $E/N = 49$ Td**

E/N, Td	Elastic, power/N, eV m^3/s	Inelastic, power/N, eV m^3/s
49	0.1492×10^{-15}	0.5087×10^{-14}

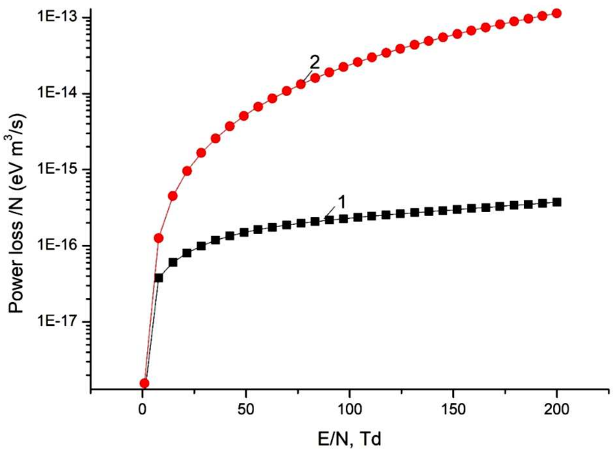

Fig. 8. Dependences of the specific discharge power losses in elastic (*1*) and inelastic (*2*) electron collisions with mercury dibromide, mercury diiodide, and mercury dichloride molecules and helium atoms on the reduced electric field strength E/N in the plasma based on the vapor mixture $HgI_2 : HgBr_2 : HgCl_2 : He = 126.2$ Pa : 449.4 Pa : 505.6 Pa : 128000 Pa with the total mixture pressure $P = 129131.2$ Pa

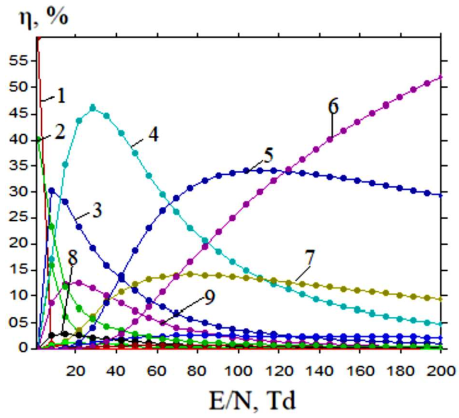

Fig. 9. Dependences of the specific discharge power losses in electron collisions with mercury dihalide molecules and helium atoms on the reduced electric field strength E/N in the plasma based on the vapor mixture $HgI_2 : HgBr_2 : HgCl_2 : He = 126.2$ Pa : 449.4 Pa : 505.6 Pa : 128000 Pa with the total mixture pressure $P = 129131.2$ Pa for various processes: elastic electron scattering by helium atoms (*1*), vibrational excitation of mercury dibromide molecules (the threshold energy $E_{th} = 0.035$ eV) (*2*), dissociative excitation of the $X^2\Sigma^+_{1/2}$ state of HgBr molecules ($E_{th} = 5.00$ eV) (*3*), excitation of the $HgBr_2(D)$ state of $HgBr_2$ molecules ($E_{th} = 7.86$ eV) (*4*), excitation of helium atoms ($E_{th} = 19.80$ eV) (*5*), ionization of helium atoms (*6*), ionization of mercury dibromide molecules ($E_{th} = 8.54$ eV) (*7*), dissociative excitation of the $B^2\Sigma^+_{1/2}$ state of HgI molecules ($E_{th} = 5.32$ eV) (*8*), dissociative excitation of the $B^2\Sigma^+_{1/2}$ state of HgBr molecules ($E_{th} = 6.40$ eV) (*9*)

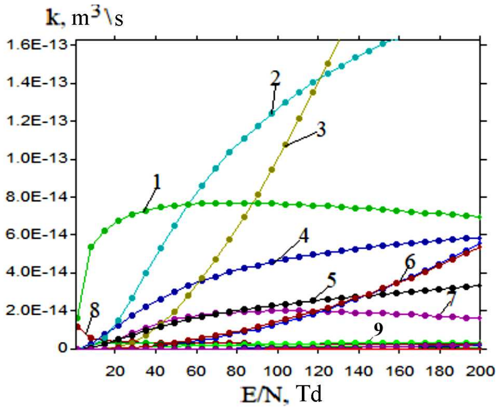

Fig. 10. Dependences of the rate constants of electron collisions with the components of the gas-discharge plasma based on the vapor mixture $HgI_2 : HgBr_2 : HgCl_2 : He =$ $= 126.2$ Pa : 449.4 Pa : 505.6 Pa : 128000 Pa with the total mixture pressure $P = 129131.2$ Pa on the parameter E/N for various processes: elastic electron scattering by helium atoms (*1*), excitation of the $HgBr_2(D)$ state of $HgBr_2$ molecules (the threshold energy $E_{th} = 7.86$ eV) (*2*), ionization of mercury dibromide molecules ($E_{th} = 8.54$ eV) (*3*), dissociative excitation of the $X^2\Sigma^+_{1/2}$ state of HgBr* molecules ($E_{th} = 5.00$ eV) (*4*), dissociative excitation of the $B^2\Sigma^+_{1/2}$ state of HgI molecules ($E_{th} = 5.32$ eV) (*5*), ionization of mercury diiodide ($E_{th} = 10.00$ eV) and mercury dibromide ($E_{th} = 11.40$ eV) molecules (*6*), dissociative excitation of the $B^2\Sigma^+_{1/2}$ state of HgBr molecules ($E_{th} = 6.40$ eV) (*7*), vibrational excitation of mercury dibromide molecules* ($E_{th} =$ $= 0.035$ eV) (*8*), dissociative excitation of the $B^2\Sigma^+_{1/2}$ state of HgCl molecules ($E_{th} = 6.49$ eV) (*9*)

of mercury monoiodide and mercury monochloride molecules, respectively. With a further increase in the reduced electric field strength E/N, the specific discharge power losses for mercury halides decrease. At the experimental reduced field strength $E/N = 49$ Td, the fractions of the specific discharge power for the $B^2\Sigma^+_{1/2}$ state were 7.2% for $HgBr_2$, 1.4% for HgI_2, 0.7% for $HgCl_2$, and 37.4% for $HgBr_2$ (D).

In Fig. 10, the dependences of the rate constants of electron collisions with various gas-discharge plasma components in the mixture $HgI_2 : HgBr_2 : HgCl_2 :$ $: He = 126.2$ Pa : 499.4 Pa : 505.6 Pa : 128000 Pa on the parameter E/N are depicted. The rate constants of dissociative excitation of the $B^2\Sigma^+_{1/2}$ state of mercury monobromide, monoiodide, and monochloride exciplex molecules by electrons reached maximum values of 2.0×10^{-14} m^3/s (at $E/N = 103.9$ Td, curve *7*), 3.3×10^{-14} m^3/s (at $E/N = 200$ Td, curve *5*), and 3.4×10^{-15} m^3/s (at $E/N = 200$ Td, curve *9*). The rate constant for the excitation of the $HgBr_2(D)$ state of $HgBr_2$ molecules (a threshold energy of 7.86 eV) equals 1.8×10^{-13} m^3/s (curve *2*) for the reduced electric field strength $E/N = 200$ Td.

3.2. Discussion of the results

The spectral bands are likely emitted due to the following reactions [23, 24, 26–28]:

$$HgX_2 + e \rightarrow HgX_2(^{3,1}\Sigma^+_u) \rightarrow$$
$$\rightarrow HgX(B^2\Sigma^+_{1/2}) + X + e, \quad (1)$$
$$HgX_2 + e \rightarrow HgX_2(^{3,1}\Sigma^+_u) \rightarrow HgX(B^2\Sigma^+_{1/2}) + X, \quad (2)$$
$$HgX_2 + e \rightarrow HgX_2(D) \rightarrow$$
$$\rightarrow HgX(C^2\Pi_{1/2}, D^2\Pi_{3/2}) + X + e, \quad (3)$$
$$HgX(C^2\Pi_{1/2}, D^2\Pi_{3/2}) + M \rightarrow$$
$$\rightarrow HgX(B^2\Sigma^+_{1/2}) + M + \Delta E_{1,2}, \quad (4)$$
$$HgX_2 + e \rightarrow HgX_2(^{3,1}\Sigma^+_u) \rightarrow$$
$$\rightarrow HgX(X^2\Sigma^+_{1/2}) + X + e, \quad (5)$$
$$HgX(B^2\Sigma^+_{1/2}) \rightarrow HgX(X^2\Sigma^+_{1/2}) + h\nu, \quad (6)$$
$$\lambda_{max} = 444 \text{ nm}, \lambda_{max} = 502 \text{ nm, and } \lambda_{max} = 557 \text{ nm},$$
$$HgX(B^2\Sigma^+_{1/2}) + M \rightarrow HgX(X^2\Sigma^+_{1/2}) + M, \quad (7)$$

where: X is a halogen (X = I, Br, Cl), M denotes molecules or atoms that quench the $B^2\Sigma^+_{1/2}$ state, the $C^2\Pi_{1/2}$ and $D^2\Pi_{3/2}$ states are the excited states of mercury monohalide exciplex molecules (HgX_2, He), and $\Delta E_{1,2}$ is the energy difference in reaction (4).

Reactions (1) and (2) are the main sources of the formation of HgX* exciplex molecules [23, 24, 29, 30]. Their rate constants are $k = 1.371 \times 10^{-14}$ m^3/s (HgI*), 1.536×10^{-14} m^3/s (HgBr*), and $1.468 \times$ $\times 10^{-15}$ m^3/s (HgCl*) (see Table 3) for our experimental conditions at the reduced electric field strength $E/N = 49$ Td.

In addition, mercury monohalide exciplex molecules are formed in reactions (3) and (4) due to the electron excitation of HgI_2, $HgBr_2$, and $HgCl_2$ molecules into the D state [30]. The rate constant equals 6.5×10^{-14} m^3/s for $HgBr_2$ molecules (Table 3). This state of mercury dihalide molecules is the sum of all states with energies between the threshold and ionization energies. Emission from the D states of

Table 3. **Rate constants for electron excitation of the $B^2\Sigma^+_{1/2}$ states of HgCl (k_{HgCl^*}), HgI (k_{HgI^*}), and HgBr (k_{HgBr^*}) exciplex molecules, electron excitation of the D state of mercury dibromide k_{HgBr_2}(D), electron excitation of the 2^3S energy level of He atoms (k_{He^*}), helium ionization (k_{He^+}), and elastic electron scattering by helium atoms (k_g) in the vapor mixture $HgI_2 : HgBr_2 : HgCl_2 : He =$ = 126.2 Pa : 449.4 Pa : 505.6 Pa : 128000 Pa with the total mixture pressure $P = 129131.2$ Pa at the reduced electric field strength $E/N = 49$ Td**

E/N, Td	$k_{HgCl^*} \times 10^{+14}$, m^3/s $\lambda = 557$ nm	$k_{HgI^*} \times 10^{+13}$, m^3/s $\lambda = 444$ nm	$k_{HgBr^*} \times 10^{+13}$, m^3/s $\lambda = 502$ nm	$k_{HgBr_2}(D) \times 10^{+13}$, m^3/s	$k_r \times 10^{+13}$, m^3/s	$k_{He^*} \times 10^{+16}$, m^3/s	$k_{He^+} \times 10^{+16}$, m^3/s
	$HgI_2 : HgBr_2 : HgCl_2$				He		He
49	0.1468	0.1371	0.1536	0.6510	0.7568	0.5009	0.1112

HgX_2 molecules is not observed because these states predissociate with the formation of mercury monohalide molecules in the C and D states. Emission from the C and D states of HgI_2, $HgBr_2$, and $HgCl_2$ molecules was not observed under our experimental conditions due to a high efficiency of the quenching process (4). (It is known that the product of the rate constant of the helium quenching of the $C^2\Pi_{1/2}$ state of mercury monoiodide molecules and the lifetime equals 4.2×10^{-18} cm^3, and the quenching process of the (C, D) states by mercury dihalides can occur more efficiently [31, 32].) The population of those states is transferred to the $B^2\Sigma^+_{1/2}$ state of HgI_2, $HgBr_2$, and $HgCl_2$ molecules or to other non-optical channels [33]. The collision reaction of mercury dihalide molecules with electrons [Eq. (5)] is a channel for the formation of mercury monohalide molecules in the ground state $X^2\Sigma^+_{1/2}$; its rate constant equals 3.0×10^{-14} m^3/s (Fig. 10, curve *4*). The electronic-vibrational transitions $B^2\Sigma^+_{1/2} \rightarrow X^2\Sigma^+_{1/2}$ of HgI_2, $HgBr_2$. and $HgCl_2$ molecules lead to the emission of spectral bands with the maximum intensity at the wavelengths $\lambda_{max} = 443$, 502, and 557 nm, respectively [reaction (6)]. In quenching reaction (7), an electronic-vibrational transition of mercury dihalide molecules into their ground state without radiation takes place. The rate constant of this process for the helium quenching of the $B^2\Sigma^+_{1/2}$ state of the mercury monoiodide and monobromide molecules equals $k = 1 \times 10^{-21}$ and $k < 2 \times 10^{-21}$ m^3 /s, respectively [34], and for the helium quenching of the $B^2\Sigma^+_{1/2}$ state of the mercury monoiodide and monobromide molecules by mercury dihalides, $k = 1.1 \times 10^{-16}$ and 3×10^{-16} m^3/s, respectively [35].

A drastic increase in the radiation intensity on the long-wavelength spectral side and its slow decrease on the short-wavelength side (Fig. 3) is explained by the behavior of the potential curves (the excited $B^2\Sigma^+_{1/2}$ state is shifted towards larger internuclear distances as compared to the $X^2\Sigma^+_{1/2}$ state) and the population relaxation processes at the upper vibrational levels of the excited electronic state, which occur faster than the electronic-vibrational transition into the ground $X^2\Sigma^+_{1/2}$ state [36, 37]. The ratio between the radiation intensities of mercury monohalide molecules (Fig. 3) is explained mainly by the ratios between the excitation rate constants for the $B^2 \sum^+_{1,2}$ state of mercury monohalides (Table 3) during their dissociative excitation by discharge electrons upon collision with mercury dihalides in reactions (1) and (2). A higher radiation intensity of HgCl* molecules (Fig. 3, *b*) than that of those molecules in Fig. 3, *a* is probably due to the larger rate constants in the quenching process [reaction (4)]. Unfortunately, the corresponding values are not known from available literature.

The dependence of the radiation power on the partial helium pressure (Fig. 4) is governed, first of all, by the following processes: an increase in the electron concentration as the partial helium pressure in the mixture increases, a variation in the fraction of discharge energy spent on heating the working mixture, changes in the average electron energy and the excitation rate constants for the HgI*, HgBr*, and HgCl* molecules, depending on the parameter E/N, and the quenching of the $B^2\Sigma^+_{1/2}$ state of the HgI, HgBr, and HgCl molecules upon collisions with helium atoms and mercury dihalide molecules. As the partial helium pressure increases, the value of the parameter E/N decreases. As a result, the specific discharge power losses grow due to the elastic scattering of electrons by atoms and molecules (Fig. 9, curve *1*); accordingly, the partial pressure of HgI_2, $HgBr_2$, and $HgCl_2$ vapors and the radiation power of HgI^*, $HgBr^*$, and $HgCl^*$ molecules increase. In addition, a higher radiation power at greater partial pressures of helium and HgI_2, $HgBr_2$, and $HgCl_2$ vapors also contributes to an increase in the electron concentration, which rises with increasing concentrations of the components in the working mixture [38]. The presence of a maximum and a subsequent drop in the radiation power of HgI^*, $HgBr^*$, and $HgCl^*$ exciplex molecules as the partial helium pressure increases (which diminishes the reduced electric field strength) is associated with a decrease in the fraction of discharge energy spent on exciting their $B^2\Sigma^+_{1/2}$ state (Fig. 9), and their excitation rate constants (Fig. 10), as well as with the quenching of this state of mercury monohalide molecules upon collisions with helium atoms [38].

The temperature dependence of the radiation power (Fig. 5) is explained by the temperature dependence of the vapor pressures of mercury dihalides (and, accordingly, their concentrations in the plasma) [17]. Furthermore, as the concentration of mercury dihalide molecules increases, the concentrations of mercury monohalide exciplex molecules HgI^*, $HgBr^*$, and $HgCl^*$ and the number of photons that they emit grow, which increases the radiation power (see reactions (1), (2), (4), and (6)). At a temperature of 150 °C, an equilibrium is reached between the processes that increase the radiation power and the quenching process during collisions of mercury monohalide molecules in the $B^2\Sigma^+_{1/2}$ energy state [reaction (7)]. If the temperature increases further, the influence of the quenching process on the radiation power prevails, and the latter decreases.

The dependence of the radiation power on the voltage-pulse amplitude (Fig. 6) is explained by the dependence of the specific discharge power losses during electron collisions with mercury dihalide molecules and helium atoms on the reduced electric field strength in the plasma. As the amplitude of voltage pulses increases, the reduced electric field strength increases; accordingly, the losses for the excitation of mercury monohalide exciplex molecules increase until their maximum values are attained. Then, if the reduced electric field strength grows further, those losses decrease, which corresponds to the dependence of the radiation power on the voltage-pulse amplitude (Fig. 9, curves *3*, *4*, *8*, and *9*).

4. Conclusions

To summarize, as a result of our studies of the optical emission and the parameters of the barrier discharge plasma based on a vapor mixture of three mercury dihalides ($HgI_2/HgBr_2/HgCl_2$) and helium, we revealed the simultaneous emission of three bands in the violet-blue, blue-green, and green spectral intervals with emission maxima at the wavelengths λ_{max} = 444, 502, and 557 nm, respectively. The following integral characteristics have been determined: the dependences of the average radiation power on the partial pressure of the helium buffer gas, the mixture temperature, and the amplitude of the voltage pulses supplied by an external source. The transport and energy parameters of electrons in the gas-discharge plasma and their dependences on the reduced electric field strength and the excitation rate constants of the $B^2\Sigma^+_{1/2}$ exciplex state of mercury monoiodide, monobromide, and monochloride molecules in the gas-discharge plasma were determined. Regularities in the radiation power dependences on the partial pressure of the helium buffer gas, the mixture temperature, and the voltage-pulse amplitude have been found.

Based on the carried out research, a new excilamp can be created, which simultaneously emits three spectral bands in the visible spectral interval and which can be used in scientific research and medicine, as a new gas-discharge light source for technological renewal and development of greenhouse farming, in biotechnology, for more effective management of photosynthesis, growth, and development of plants and algae, in the seawater desalination technology, and in more energy-efficient drying methods in industry.

1. G.Z. Zissis, S.K. Kitsinelis. State of art on the science and technology of electrical light sources: From the past to the future. *J. Phys. D* **42**, 173001 (2009).
2. U.K. Kogelschatz. Dielectric barrier discharges: their history, discharge physics and industrial applications. *Plasma Chem. Plasma Process.* **23**, 1 (2003).
3. A.M. Boichenko, M.I. Lomaev, A.N. Panchenko *et al. Ultraviolet and Vacuum Ultraviolet Excilamps: Physics, Engineering, and Applications* (STT, 2011).

4. A.N. Malinin. Excitation of mercury monohalides in the plasma of pulse-periodic discharge in mixtures of mercury dihalides and rare gases. *Laser Phys.* **7**, 1032 (1997).
5. A.N. Malinin. The main characteristics of the plasma of pulse glow discharge in mixtures of mercury dihalides and rare gases. *Laser Phys.* **8**, 395 (1998).
6. A.A. Malinina, A.N. Malinin. Optical characteristics and parameters of gas-discharge plasma in a mixture of mercury dibromide vapor with neon. *Plasma Phys. Rep.* **39**, 1035 (2013).
7. A. Malinina. Diagnostics of optical characteristics and parameters of gas-discharge plasma based on mercury diiodide and helium mixture. *Open J. Appl. Sci.* **5**, 826 (2015).
8. A.A. Malinina, A.N. Malinin. Optical characteristics of a gas discharge plasma based on a mixture of mercury diiodide vapor, nitrogen, and helium. *J. Appl. Spectrosc.* **83**, 592 (2016).
9. A.O. Malinina, O.K. Shuaibov, O.M. Malinin. Mechanism of growth of the intensity of radiation emitted in the blue-violet spectral interval by gas-discharge plasma generated in the mixtures of mercury diiodide vapor, xenon, and neon. *Ukr. Fiz. Zh.* **62**, 590 (2017) (in Ukrainian).
10. A.A. Malinina, R.V. Hrytsak. Optical characteristics and parameters of gas-discharge plasma on mixtures of mercury dichloride vapor and neon. *Probl. At. Sci. Technol.* **4**, 124 (2019).
11. A.O. Malinina, O.K. Shuaibov, O.M. Malinin. Mechanism enhancing the emission power of gas-discharge lamps based on mixtures of neon, nitrogen, and mercury dichloride vapor in the blue-green spectral interval. *Ukr. Fiz. Zh.* **64**, 803 (2019) (in Ukrainian).
12. A.O. Malinina, O.K. Shuaib. Radiation characteristics and parameters of gas-discharge plasma in a mixture of mercury dichloride vapor and nitrogen. *Zh. Fiz. Dosl.* **24**, 1401 (2020) (in Ukrainian).
13. A.N. Malinin, K.B. Molnar, A.O. Malinina. Parameters of gas-discharge plasma of barrier discharge on mixtures of vapours of diiodide, dibromide and mercury dichloride with helium. *Sci. Herald Uzhhorod Univ. Ser. Phys.* **50**, 1 (2021).
14. C. D'Avino, S. Gutiérrez, M.J. Feldhaus, M. Tomás-Gamasa, J.L. Mascareñas. Intracellular synthesis of indoles enabled by visible-light photocatalysis. *J. Am. Chem. Soc.* **146**, 2895 (2024).
15. Guangxin Lv, Yaodong Tu, J.H. Zhang, Gang Chen. Photomolecular effect: visible light interaction with air-water interface. *Proc. Natl. Acad. Sci. USA* **121**, e2320844121 (2024).
16. Ming Zhang, Wei Liu, Cai-Jun Zheng, Kai Wang, Yi-Zhong Shi, Xing Li, Hui Lin, Si-Lu Tao, Xiao-Hong Zhang. Tricomponent exciplex emitter realizing over 20% external quantum efficiency in organic light-emitting diode with multiple reverse intersystem crossing channels. *Adv. Sci.* **6**, 1801938 (2019).
17. A.I. Efimov, L.P. Belorukova, I.V. Vasil'kova, V.P. Chechev. *Properties of Inorganic Compounds* (Khimiya, 1983).
18. R.W. Pearse, A.G. Gaydon. *The Identification of Molecular Spectra* (Chapman and Hall, 1963).
19. R.H. Huddlestone, S.L. Leonard. *Plasma Diagnostic Techniques* (Academic Press, 1965).
20. G.J.M. Hagelaar, L.C. Pitchford. Solving the Boltzmann equation to obtain electron transport coefficients and rate coefficients for fluid models. *Plasma Sources Sci. Technol.* **14**, 722 (2005).
21. *BOLSIG+. Electron Boltzmann equation solver.* http://www.bolsig.laplace.univ-tlse.fr.
22. W.L. Nighan, R.T. Brown. Kinetic processes in the $HgBr/HgBr_2$ dissociation laser. *J. Appl. Phys.* **53**, 7201 (1982).
23. V. Kushawaha, M. Mahmood. Electron impact dissociation of HgX_2 (X = Cl, Br, I). *J. Appl. Phys.* **62**, 2173 (1987).
24. A.N. Malinin. Excitation of the $B^2\Sigma^+_{1/2}$ state of mercury monohalides by electron impact. *Laser Phys.* **7**, 1168 (1997).
25. M.I. Lomaev, V.S. Skakun, E.A. Sosnin, V.F. Tarasenko, D.V. Shitts, M.V. Erofeev. Excilamps: efficient sources of spontaneous UV and VUV radiation. *Phys.-Usp.* **46**, 193 (2003).
26. E.W. McDaniel, W.L. Nighan. *Gas Lasers* (Academic Press, 1982).
27. C.K. Rhodes. *Excimer Lasers* (Springer, 1979).
28. M. Jakob. Ultraviolet absorption cross sections of HgI_2, $HgBr_2$, and tin(II) halide vapors. *J. Chem. Phys.* **64**, 4976 (1977).
29. A.N. Malinin, A.K. Shuaibov, V.S. Shevera. Dissociative excitation of the $B^2\Sigma^+_{1/2}$ states of mercury monohalides by electron impact. *Sov. J. Quantum Electron.* **10**, 1495 (1983).
30. W.L. Nighan, R.T. Brown. Kinetic processes in the $HgBr(B\rightarrow X)/HgBr_2$ dissociation laser. *J. Appl. Phys.* **53**, 7201 (1982).
31. A. Malinina. *Optical Characteristics of Gas-Discharge Plasma in Mixtures of Mercury Dibromide Vapor with Gases* (Cambridge Scholars Publishing, 2020).
32. R.W. Waynant, J.G. Iden. HgX(B) radiative lifetime by fast photolysis of HgX_2 (X = Br, I). *Appl. Phys. Lett.* **33**, 708 (1978).
33. V.V. Datsyuk, I.A. Izmailov, V.V. Naumov, A.V. Kochelap. Direct electron-impact mechanism of excitation of mercury monobromide in a double-pulse dielectric-barrier-discharge HgBr lamp. *Plasma Sources Sci. Technol.* **25**, 015018 (2016).
34. C. Roxlo, A. Mandl. Quenching kinetics for the $HgBr^*$ ($B^2\Sigma^+_{1/2}$) and HgI^* ($B^2\Sigma^+_{1/2}$, $C^2\Pi_{1/2}$) states. *J. Chem. Phys.* **72**, 541 (1980).
35. A.A. Malinina, A.N. Malinin. Efficiency of quenching of the $B^2\Sigma^+_{1/2}$ state of mercury monoiodide and monobromide by mercury dihalides in gas-discharge plasma in multicomponent mixtures of an exciplex radiation source. *Opt. Spectrosc.* **105**, 32 (2008).

36. R.W. Wadt. The electronic structure of HgCl and HgBr. *Appl. Phys. Lett.* **34**, 658 (1979).
37. V.V. Datsyuk, I.A. Izmailov, V.V. Naumov, V.A. Kochelap. Vibrational relaxation of excimers. *Phys.-Usp.* **41**, 379 (1998).
38. Y.P. Raizer. *Gas Discharge Physics* (Springer, 1991).

Received 05.03.26.
Translated from Ukrainian by O.I. Voitenko

О.М. Малінін, А.О. Малініна, О.К. Шуаібов, К.Б. Молнар, О.Й. Миня, Р.В. Грицак, М.О. Маргітич

ОПТИЧНІ ХАРАКТЕРИСТИКИ ВИПРОМІНЮВАННЯ ТА ПАРАМЕТРИ ПЛАЗМИ БАР'ЄРНОГО РОЗРЯДУ ДЛЯ СУМІШІ ПАРІВ ДИЙОДИДУ, ДИБРОМІДУ ТА ДИХЛОРИДУ РТУТІ З ГЕЛІЄМ

Досліджено спектральні, енергетичні характеристики випромінювання та параметри плазми імпульсно-періодичного наносекундного бар'єрного розряду атмосферного тиску на суміші парів трьох дигалогенидів ртуті (HgI_2/$HgBr_2$/$HgCl_2$) і гелію. Виявлено одночасне випромінювання спектральних смуг фіолетово-синього ($\lambda_{\text{макс.}} = 444$ нм), синьо-зеленого ($\lambda_{\text{макс.}} = 502$ нм) і зеленого ($\lambda_{\text{макс.}} = 557$ нм) діапазонів спектра. Обговорено механізм утворення ексиплексних молекул моногалогенидів ртуті (HgI*, HgBr* і HgCl*). Встановлено константи швидкості збудження ексиплексних молекул моногалогенидів ртуті. Визначено оптимальні значення приведеної напруженості електричного поля, для яких спостерігається максимальна потужність випромінювання у фіолетово-синьому, синьо-зеленому й зеленому діапазоні спектра з максимумами емісії на довжинах хвиль: 444 нм, 502 нм і 557 нм. На основі проведених досліджень може бути створена нова ексилампа, що випромінює одночасно три спектральні смуги у видимому діапазоні, яка може бути використана: у наукових дослідженнях, медицині, для технологічного оновлення та розвитку парникового господарства, в біотехнології, для більш ефективного керування фотосинтезом, ростом і розвитком рослин і водоростей, а також для покращення технології опріснення морської води і енергоефективності методів сушіння в промисловості.

Ключові слова: наносекундний бар'єрний розряд, випромінювання ексиплексних молекул, параметри плазми, моногалогениди ртуті, гелій.